Staggered-PRT Sequences for Doppler Weather Radars. Part I: Spectral Analysis Using the Autocorrelation Spectral Density

SEBASTIÁN M. TORRES AND DAVID A. WARDE

Cooperative Institute for Mesoscale Meteorological Studies, University of Oklahoma, and NOAA/OAR/National Severe Storms Laboratory, Norman, Oklahoma

(Manuscript received 1 April 2016, in final form 11 October 2016)

ABSTRACT

The autocorrelation spectral density (ASD) was introduced as a generalization of the classical periodogram-based power spectral density (PSD) and as an alternative tool for spectral analysis of uniformly sampled weather radar signals. In this paper, the ASD is applied to staggered pulse repetition time (PRT) sequences and is related to both the PSD and the ASD of the underlying uniform-PRT sequence. An unbiased autocorrelation estimator based on the ASD is introduced for use with staggered-PRT sequences when spectral processing is required. Finally, the strengths and limitations of the ASD for spectral analysis of staggered-PRT sequences are illustrated using simulated and real data.

1. Introduction

Weather observations using pulsed Doppler radars are limited by inherent range and velocity ambiguities. The Doppler dilemma states that, for radars operating with a uniform pulse repetition time (PRT), the maximum unambiguous range (r_a) and maximum unambiguous velocity (v_a) are inversely coupled: improving one typically results in worsening the other (Doviak and Zrnić 1993). One way to address this limitation is through the use of nonuniform transmitter sequences. Sirmans et al. (1976) first proposed pulse trains with alternating (or staggered) PRTs on weather radars to extend v_a without reducing r_a. Compared to the conventional processing of uniformly sampled signals, the staggered-PRT technique extends the maximum unambiguous velocity by considering Doppler velocity estimates from sample pairs spaced by two different PRTs (T_1 and T_2). Because the PRTs are different, so are their corresponding maximum unambiguous velocities (v_{a1} and v_{a2}); thus, Doppler velocity estimates (v_1 and v_2) from each set of sample pairs alias in different ways and provide a means to identify the correct way to dealias them over a much larger interval. That is, for a PRT ratio of the form $T_1/T_2 = n_1/n_2$ (where n_1 and n_2 are small positive integers that share no common factors except 1), the extended maximum unambiguous velocity using the staggered-PRT technique is $v_a = n_1 v_{a1} = n_2 v_{a2}$ (Torres et al. 2004).

A similar technique was proposed by Dazhang et al. (1984), whereby a train of pulses with (uniform) PRT of T_1 is followed by another train of pulses with PRT of T_2. This dual pulse repetition frequency (PRF) technique has a practical advantage over staggered PRT in that it is amenable to conventional ground clutter filters. However, dual PRF is prone to velocity-dealiasing errors if there is shear in the radar resolution volume, which is likely for scanning antennas and small-scale weather phenomena, such as tornados. The staggered-PRT technique is not as prone to shear-induced velocity-dealiasing errors and provides an additional advantage in the way range overlaid echoes are handled (Doviak and Zrnić 1993; Warde and Torres 2009). Other techniques have been proposed that use more than two interlaced PRTs and allow an even greater extension of v_a (e.g., Chornoboy and Weber 1994; Pirttilä et al. 2005; Cho 2005; Tabary et al. 2006; Torres et al. 2010). However, their increased complexity makes them more appealing for use on radars that operate at shorter wavelengths or that cannot operate with short PRTs, for which the performance of the staggered-PRT technique may be inadequate to resolve the exacerbated range and velocity ambiguities (e.g., Tabary et al. 2005).

To achieve a good balance between performance and complexity, the U.S. National Weather Service (NWS)

Corresponding author e-mail: Sebastián Torres, sebastian.torres@noaa.gov

DOI: 10.1175/JTECH-D-16-0071.1

has adopted the staggered-PRT technique for future operational implementation on their S-band Weather Surveillance Radar-1988 Doppler (WSR-88D) network (Warde et al. 2014). One of the main challenges of developing an operational implementation of the staggered-PRT technique has been the design of effective ground clutter filters, which is a nontrivial task due to the inherent nonuniform sampling of the signals. When left unaddressed, contamination from ground returns can greatly affect the performance of weather radars by severely biasing all radar variables and potentially impeding the recognition of weather phenomena (Doviak and Zrnić 1993). Much research has been devoted to the design of effective ground clutter filters for weather radars; the reader is referred to Hubbert et al. (2009) and Moisseev and Chandrasekar (2009) for excellent literature reviews on ground clutter filters for weather radars. Recently, the novel Clutter Environment Analysis using Adaptive Processing (CLEAN-AP[1]) filter (Torres and Warde 2014) was identified as a candidate for operational implementation on the WSR-88D. At the core of the CLEAN-AP filter is the autocorrelation spectral density (ASD) introduced by Warde and Torres (2014) as an extension of the classical periodogram-based power spectral density (PSD). Unlike the PSD, the ASD includes spectral phase information that allows the robust identification of narrowband signals, such as those typical of ground clutter returns.

In this paper, we apply the ASD to staggered-PRT sequences and relate them to the PSD and to the ASD of the underlying uniform-PRT sequence. Further, we derive autocorrelation estimators that are compatible with staggered-PRT processing and explore the utility of the ASD for spectral analysis of staggered-PRT sequences. This work is used by Warde and Torres (2016, manuscript submitted to *J. Atmos. Oceanic Technol.*, hereafter Part II) as a basis for integrating the CLEAN-AP filter into the WSR-88D staggered-PRT algorithm.

2. The ASD of staggered-PRT sequences

The ASD was introduced by Warde and Torres (2014) as a generalization of the PSD and as an alternative tool for spectral analysis of weather radar signals. In this section, the theory of the ASD for uniformly sampled signals is reviewed and the ASD is applied to staggered-PRT sequences.

Consider a uniformly sampled complex-valued sequence $\{V(kT_s)\}$ with $0 \le k < K$, where K is the length of the sequence and T_s is the sampling period (i.e., the PRT). Assume that there are enough samples such that $l+1$ subsequences with M samples each can be formed: $\{V(mT_s)\}$, $\{V[(m+1)T_s]\}$, ... , and $\{V[(m+l)T_s]\}$, where m and l are positive integers, and $0 \le m < M$. The lag-l ASD is defined as

$$\hat{S}_l(f) = \frac{T_s}{M} F_0^*(f) F_l(f), \quad -(2T_s)^{-1} < f < (2T_s)^{-1}, \qquad (1)$$

where f is Doppler frequency and the superscript asterisk (*) denotes complex conjugation. In this formulation, F_i ($i = 0$ or l) is the discrete-time Fourier transform (DTFT) of the M-sample signal subsequence after time shifting by iT_s and windowing with a power-preserving data window (d) such that $\sum_{m=0}^{M-1} d^2(mT_s) = M$; that is,

$$F_i(f) = \sum_{m=0}^{M-1} d(mT_s) V[(m+i)T_s] e^{-j2\pi f T_s m}. \qquad (2)$$

It was proven by Warde and Torres (2014) that the expected value of the lag-l ASD is the circular convolution (denoted by $\circledast$) between a complex spectrum with magnitude given by the PSD and with linear phase given by $2\pi f T_s l$ and the DTFT of the lag window[2] (W); that is,

$$E[\hat{S}_l(f)] = [S(f) e^{j2\pi f T_s l}] \circledast W(f). \qquad (3)$$

The ASD conveys explicit phase information that reveals spectral signatures not obvious in the PSD. In fact, the effects of data windowing on the phase of the ASD can be exploited to robustly identify narrowband signals and improve the mitigation of ground clutter contamination on weather radars (Torres and Warde 2014).

To apply the ASD to staggered-PRT sequences, consider an underlying uniform-PRT sequence $\{V(kT_u)\}$, where T_u is the sampling period, such that staggered-PRT sampling can be obtained by decimation; that is, the PRTs in the staggered-PRT sampling scheme are integer multiples of T_u: $T_1 = n_1 T_u$ and $T_2 = n_2 T_u$. In addition, the staggered-PRT ratio is $T_1/T_2 = n_1/n_2$, and the period of the staggered-PRT sampling scheme is $T_s = T_1 + T_2 = (n_1 + n_2)T_u = n_s T_u$ with $n_s = n_1 + n_2$. As before, we can form an arbitrary number of M-sample subsequences: $\{V(mT_s)\}$, $\{V[(m + n_1/n_s)T_s]\}$, $\{V[(m+1)T_s]\}$, $\{V[(m + 1 + n_1/n_s)T_s]\}$, etc., where $0 \le m < M$. Here, we are purposely forcing a sampling

[1] CLEAN-AP ©2009 Board of Regents of the University of Oklahoma.

[2] The lag window is the autocorrelation of the data window at a particular lag l (Doviak and Zrnić 1993).

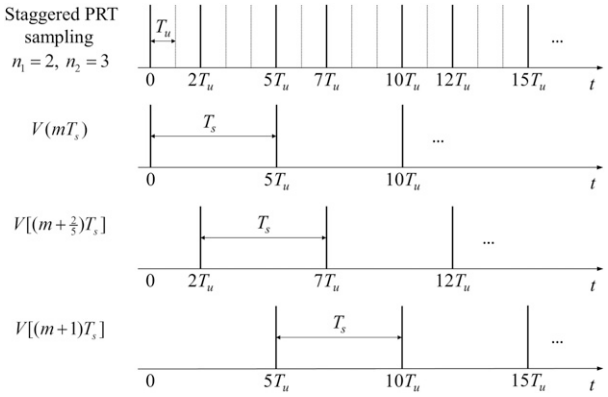

FIG. 1. Example of staggered-PRT sampling with $n_1 = 2$ and $n_2 = 3$, i.e., $T_s = 5T_u$. (top) Staggered-PRT sampling (solid lines) via decimation of an underlying uniform-PRT sequence with sampling period T_u (dotted lines). The remaining panels illustrate the first three uniform-PRT subsequences with sampling period T_s that can be obtained from the staggered-PRT sequence.

period of T_s that leads to fractional indices; however, these are equivalent to integer indices for the underlying sampling period T_u. Figure 1 illustrates this process for a staggered-PRT ratio of 2/3 (i.e., $T_s = 5T_u$). With these definitions, we can use (2) to compute F_o, F_{n_1/n_s}, F_1, F_{1+n_1/n_s}, etc., by allowing i to take both fractional and integer values, that is, $i = 0, n_1/n_s, 1, 1 + n_1/n_s \ldots$. In turn, these can be paired in different ways to compute the ASD of a staggered-PRT sequence for fractional or integer lags as

$$\hat{S}_{l-l'}(f) = \frac{T_s}{M} F_{l'}^*(f) F_l(f), \quad -(2T_s)^{-1} < f < (2T_s)^{-1}. \quad (4)$$

For example, the ASD for lags n_1/n_s, n_2/n_s, and 1 can be computed as $\hat{S}_{n_1/n_s-0}$, $\hat{S}_{1-n_1/n_s}$, and $\hat{S}_{1-0}$, respectively. These particular lags will be the focus of section 4 on using the ASD for spectral analysis of staggered-PRT sequences.

Because of the similarities between (1) and (4), the properties derived for the ASD of uniform-PRT sequences can be readily extended to the ASD of staggered-PRT sequences. Warde and Torres [2014, (A6)] showed that the expected value of the lag-l ASD is

$$E[\hat{S}_l(f)] = T_s \sum_n R[(n+l)T_s] w(nT_s) e^{-j2\pi f T_s n}, \quad (5)$$

where R is the autocorrelation function, w is the lag window, and n spans the set of integers. This expression can be naturally extended to the lag-$(l - l')$ ASD in (4) as

$$E[\hat{S}_{l-l'}(f)] = T_s \sum_n R[(n + l - l')T_s] w(nT_s) e^{-j2\pi f T_s n}. \quad (6)$$

Because we are interested in expressing the expected value of the ASD of a staggered-PRT sequence in terms of the ASD of its underlying uniform-PRT sequence, let us make the substitution $T_s = n_s T_u$ and the change of variable $n' = nn_s$ to obtain

$$E[\hat{S}_{l-l'}(f)] = n_s T_u \sum_{n'} R[n' T_u + (l - l') n_s T_u] w(n' T_u) e^{-j2\pi f T_u n'}. \quad (7)$$

Note that n' consists only of the integer multiples of n_s, so the previous equation can be modified by adding a periodic train of Kronecker deltas with period T_s and switching back to the original summation index n,

$$E[\hat{S}_{l-l'}(f)] = n_s T_u \sum_n R[nT_u + (l - l') n_s T_u] w(nT_u) e^{-j2\pi f T_u n} \times \sum_k \delta[(n - kn_s)T_u], \quad (8)$$

where, as before, n spans the set of integers. The summation on the right-hand side of this equation can be recognized as the DTFT of the sequence

$$x(nT_u) = R[nT_u + (l - l') n_s T_u] w(nT_u) \sum_k \delta[(n - kn_s)T_u], \quad (9)$$

which can be obtained using well-known properties as

$$X(f) = \mathcal{F}\{R[nT_u + (l - l') n_s T_u]\} \circledast \mathcal{F}\{w(nT_u)\} \circledast \mathcal{F}\left\{ \sum_k \delta[(n - kn_s)T_u] \right\}$$
$$= e^{j2\pi f T_u n_s (l - l')} \mathcal{F}\{R(nT_u)\} \circledast \mathcal{F}\{w(nT_u)\} \circledast \frac{1}{n_s} \sum_k \delta\left(f - \frac{k}{n_s T_u} \right), \quad (10)$$

where $\mathcal{F}$ denotes the DTFT operator and $-(2T_u)^{-1} < f < (2T_u)^{-1}$. Finally, (10) can be inserted into (8), and we can use the fact that the PSD (S) is proportional to the DTFT of the autocorrelation, that is, $S(f) = T_u \mathcal{F}\{R(nT_u)\}$. Thus, the expected value of the ASD of a staggered-PRT sequence can be expressed as a

function of the PSD of its underlying uniform-PRT sequence as

$$E[\hat{S}_{l-l'}(f)] = \sum_k S(f - kf_s)e^{j2\pi(f-kf_s)T_u n_s(l-l')} \circledast W(f), \quad (11)$$

where $f_s = T_s^{-1} = (n_s T_u)^{-1}$.

It is interesting to note that in the mean and for a very large number of samples (i.e., ignoring windowing effects),

$$\lim_{M\to\infty} E[\hat{S}_{l-l'}(f)] = \sum_k S(f - kf_s)e^{j2\pi(f-kf_s)T_u n_s(l-l')}; \quad (12)$$

namely, the fractional-lag-$(l - l')$ ASD of a staggered-PRT sequence is the integer-lag-$n_s(l - l')$ ASD of its underlying uniform-PRT sequence, $S(f)e^{j2\pi f T_u[n_s(l-l')]}$, *aliased* in the interval $-f_s/2 < f < f_s/2$. Figure 2 illustrates this for a staggered-PRT sequence with a PRT ratio of 2/3 ($n_s = 5$). In this depiction, the lag-2/5 ASD of the staggered-PRT sequence is obtained as the aliased lag-2 ASD of the underlying uniform-PRT sequence. Because $f_s = f_u/5$, the Nyquist cointerval corresponding to T_u can be thought of as being divided into five subintervals that alias and combine to form the ASD of the staggered-PRT sequence (these subintervals are denoted with roman numerals in the figure). The lag-3/5 and lag-1 ASDs of the staggered-PRT sequence could be similarly obtained as aliased versions of the lag-3 and lag-5 ASDs of the underlying uniform-PRT sequence, respectively. Whereas the magnitude of these ASDs would be the same as the one in Fig. 2, their phases would be different. This is because the phases of the ASD of the underlying uniform-PRT sequence at lags 2, 3, and 5 are also different and given by $2(2\pi f T_u)$, $3(2\pi f T_u)$, and $5(2\pi f T_u)$, respectively. It is interesting to note that these phases are periodic functions of f with periods given by $5f_s/2$, $5f_s/3$, and $5f_s/5 = f_s$, respectively. Hence, the phase of the lag-5 ASD of the underlying uniform-PRT sequence is the same in each of the five f_s-wide subintervals, and they alias onto the same line to form the lag-1 ASD of the staggered-PRT sequence.

As with uniform-PRT sequences, the ASD is trivial when the number of samples is very large: its magnitude is the aliased PSD of the underlying uniform-PRT sequence, and its phase is an aliased linear function with slope proportional to $n_s(l - l')$. However, in the presence of windowing effects and for the typical numbers of samples employed on operational weather radars, the phase of the ASD is not trivial and, as will be illustrated in section 4, it provides additional information to perform spectral analysis of staggered-PRT sequences.

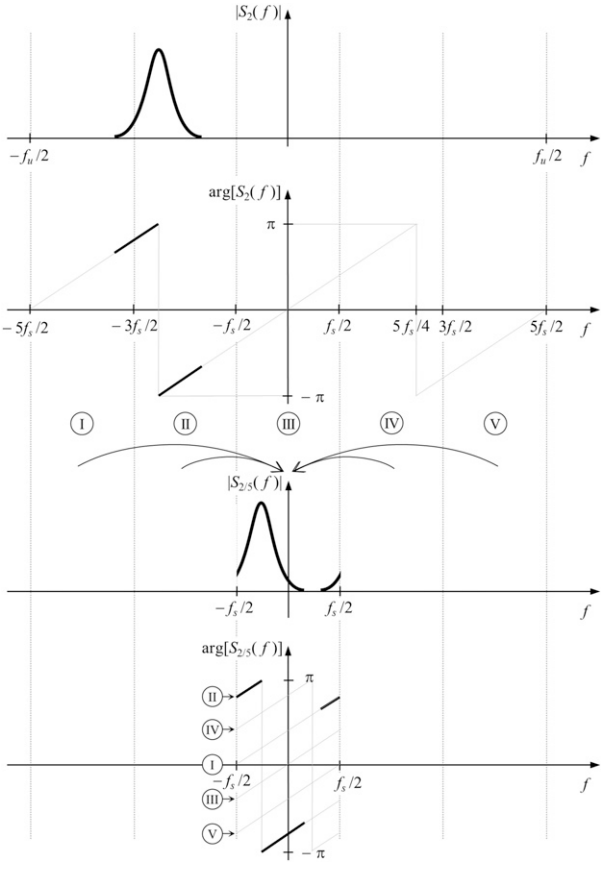

FIG. 2. (bottom two) Example of the lag-2/5 ASD for a staggered-PRT sequence with a PRT ratio of 2/3 and (top two) the corresponding lag-2 ASD for the underlying uniform-PRT sequence. Dotted vertical lines partition the Nyquist cointerval corresponding to the underlying uniform-PRT sampling into five subintervals (I–V) that alias and combine to form the ASD of the staggered-PRT sequence. Light lines labeled with roman numerals in the bottom plot correspond to the aliased ASD phases from the same subinterval in the ASD of the underlying uniform-PRT sequence.

3. Autocorrelation estimation based on the ASD

As discussed in the introduction, the staggered-PRT algorithm relies on autocorrelation estimates at lags T_1 and T_2 from which Doppler velocities are computed and used in a velocity dealiasing algorithm (Torres et al. 2004). While autocorrelation estimates can be easily obtained in the time domain, if spectral processing is needed (e.g., for ground clutter filtering purposes), it makes sense to use a frequency domain autocorrelation estimator. In this section, we introduce an ASD-based autocorrelation estimator for use with staggered-PRT sequences.

Similar to the ASD-based autocorrelation estimator introduced by Warde and Torres (2014), the autocorrelation at lag $(l - l')T_s$ can be estimated from the corresponding fractional-lag ASD estimate as

$$\hat{R}[(l-l')T_s] = \frac{1}{T_s}\int_{-f_s/2}^{f_s/2} \hat{S}_{l-l'}(f)\,df. \tag{13}$$

In practice, the ASD is estimated using the discrete Fourier transform (DFT) so that

$$F_i(k) = \sum_{m=0}^{M-1} d(m)V(m+i)e^{-j(2\pi mk/M)},$$
$$\text{where} \quad i = l \text{ or } l', \tag{14}$$

and

$$\hat{S}_{l-l'}(k) = \frac{T_s}{M}F_{l'}^*(k)F_l(k), \quad \text{for} \quad 0 \le k < M. \tag{15}$$

Thus, the lag-$(l-l')T_s$ autocorrelation can be obtained from the corresponding ASD estimate as

$$\hat{R}[(l-l')T_s] = \frac{1}{T_s M}\sum_{k=0}^{M-1} \hat{S}_{l-l'}(k). \tag{16}$$

Following the same procedure as in appendix B of Warde and Torres (2014), the expected value of the ASD-based autocorrelation estimator can be found by substituting (15) and (14) into (16); that is,

$$\begin{aligned}\hat{R}[(l-l')T_s] &= \frac{1}{M^2}\sum_{k=0}^{M-1}\sum_{m=0}^{M-1}\sum_{m'=0}^{M-1} d(m)d(m')V^*(m+l')V(m'+l)e^{-j[(2\pi k/M)(m'-m)]}\\ &= \frac{1}{M}\sum_{m=0}^{M-1} d^2(m)V^*(m+l')V(m+l),\end{aligned} \tag{17}$$

where we used the fact that the sum of the complex exponentials on k is $M\delta(m'-m)$ (Oppenheim and Schafer 2009). The previous equation shows that for a rectangular data window [i.e., $d(m) = 1$ for $0 \le m < M$], the ASD-based autocorrelation estimator is mathematically equivalent to the time-domain unbiased autocorrelation estimator. For other normalized data windows, this equivalence is lost but the ASD-based autocorrelation estimator is unbiased, that is,

$$\begin{aligned}E\{\hat{R}[(l-l')T_s]\} &= \frac{1}{M}\sum_{m=0}^{M-1} d^2(m)E[V^*(m+l')V(m+l)]\\ &= R[(l-l')T_s].\end{aligned} \tag{18}$$

Therefore, despite aliasing, the ASD of staggered-PRT sequences can be used as the basis to obtain unbiased autocorrelation estimates.

4. Spectral analysis of staggered-PRT sequences

Having defined the ASD for staggered-PRT sequences and derived a corresponding autocorrelation estimator, in this section we present a few examples to illustrate the strengths and limitations of the ASD for spectral analysis of staggered-PRT sequences.

a. Simulated data analyses

For the following examples, simulated staggered-PRT sequences are obtained by decimating a uniformly sampled sequence (i.e., the underlying uniform-PRT sequence) obtained with the simulator described by Zrnić (1975). For all cases, $T_1 = 1$ ms, $T_2 = 1.5$ ms (the PRT ratio is 2/3), $M = 32$ (the total number of samples is 65), and the radar wavelength is 10 cm; thus, the unambiguous velocities corresponding to T_u and T_s ($v_{a,u}$ and $v_{a,s}$) are 50 and 10 m s^{-1}, respectively. Figures 3–8 show the magnitude (top panels) and phase (bottom panels) of the ASD at lags 2/5 (left panels), 3/5 (middle panels), and 1 (right panels) as a function of Doppler velocity. The dashed lines in the phase plots correspond to the aliased theoretical ASD phases of the underlying uniform-PRT sequence ignoring data windowing effects: they are linear functions given by $-\pi(l-l')v/v_{a,s}$ and are aliased in the Nyquist cointerval $\pm v_{a,s}$. Note that these are mirror images of the theoretical lines in Fig. 2 because v and f are related by $v = -\lambda f/2$.

We designed the following examples with the goal of illustrating how the ASD of staggered-PRT sequences changes as signal characteristics change. We start with the simple case of a single signal and progress toward the more complex case of a combination of signals for which the use of spectral analysis is justified. Figure 3 shows the ASD of a typical staggered-PRT weather signal with a signal-to-noise ratio (SNR) of 40 dB, a mean Doppler velocity ($\overline{v}$) of 0 m s^{-1}, and a spectrum width (σ_v) of 2 m s^{-1}. Whereas these are somewhat arbitrary parameters, Fang et al. (2004) showed that the median spectrum width in most storms is less than 2 m s^{-1}. Further, the zero mean Doppler velocity is adopted to later compare this with a typical ground clutter signal. Designed as such, this first example is not very interesting: there is no aliasing of the underlying uniform-PRT sequence ASD, the magnitudes of the ASD at all lags are

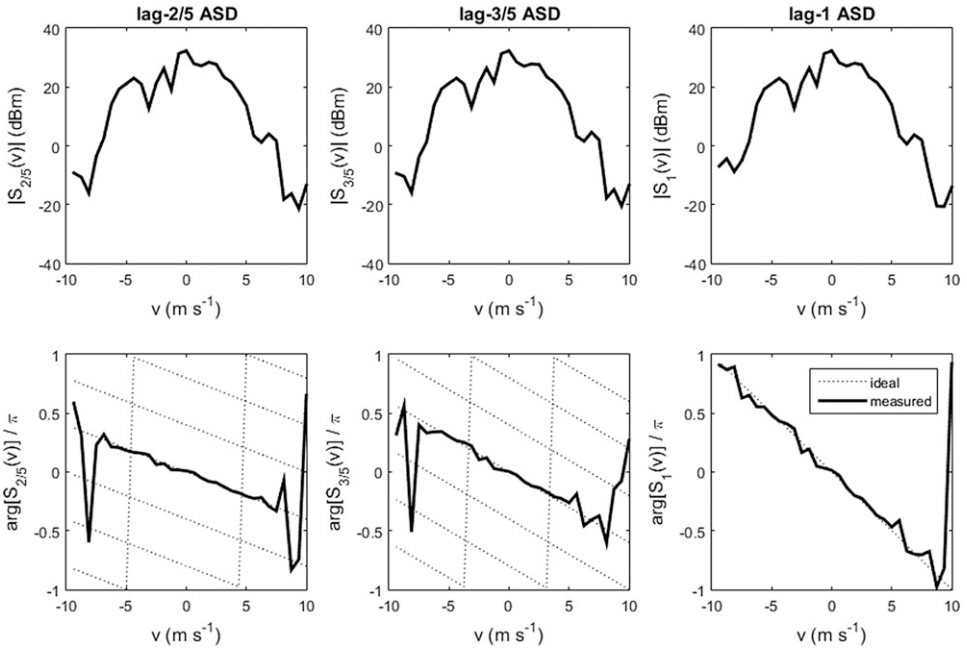

FIG. 3. (top) Magnitude and (bottom) phase of the ASD at lags (left) 2/5, (center) 3/5, and (right) 1 as a function of Doppler velocity for a simulated staggered-PRT sequence typical of weather returns. The sequence has 65 samples with $T_1 = 1$ ms and $T_2 = 1.5$ ms, the SNR is 40 dB, the mean Doppler velocity is $0\,\mathrm{m\,s^{-1}}$, and the spectrum width is $2\,\mathrm{m\,s^{-1}}$. The dotted lines in the phase plots correspond to the aliased theoretical ASD phases of the underlying uniform-PRT sequence, and the solid lines correspond to the measured ASD phases of the corresponding staggered-PRT sequence.

similar (although not identical), and there is good agreement between the theoretical and measured ASD phases. The dotted lines in the figure show where the theoretical (ignoring windowing effects) ASD phases of the underlying uniform-PRT sequence would alias. As mentioned in the previous section, the phases for integer-lag ASDs alias to the same line; however, in general, the phases for fractional-lag ASDs alias to different lines, which can be exploited to infer the location of the underlying uniform-PRT spectrum in the extended Nyquist cointerval (this will be shown in a later example). Figure 4 shows the ASD of a typical staggered-PRT ground clutter return with SNR = 40 dB and $\overline{v} = 0\,\mathrm{m\,s^{-1}}$. The spectrum width is chosen as $\sigma_v = 0.28\,\mathrm{m\,s^{-1}}$, which is the same as the one used for testing the WSR-88D ground clutter filter performance (Sirmans 1992). This case is more interesting because, for all lags, there are prominent biases in the phases of the measured ASD (compared to the theoretical lines), indicating the presence of a narrowband signal. Also, compared to the lag-1 ASD, the phases of the fractional-lag ASDs corresponding to the spectral components of the noise have markedly different behavior. That is, whereas the lag-1 ASD phases of the noise components are close to the theoretical line, those for lags 2/5 and 3/5 appear to be random. This is because the aliased spectral components of the lag n_s ASD of the underlying uniform-PRT sequence add coherently (i.e., the phases are the same) to produce the lag-1 ASD of the corresponding staggered-PRT sequence.

Figure 5 shows the ASD of a staggered-PRT sequence with SNR = 40 dB, $\overline{v} = 20\,\mathrm{m\,s^{-1}}$, and $\sigma_v = 0.28\,\mathrm{m\,s^{-1}}$. Although this is a narrowband signal with the same spectrum width as the typical ground clutter signal used in the previous example, it has a nonzero Doppler velocity so it is not representative of ground clutter returns. However, its velocity is such that it aliases to zero; thus, it would look like a typical ground clutter signal in the PSD (magnitude only). This example illustrates the power of the ASD of staggered-PRT sequences at fractional lags: while the magnitude and phase of the lag-1 ASD makes this signal look like a typical ground clutter return, the phases of the ASD at lags 2/5 and 3/5 lie on different theoretical lines and provide clear evidence that the underlying uniform-PRT signal does not have a zero mean Doppler velocity. Thus, using the phase information from the fractional-lag ASDs, it could be possible to dealias the spectrum (similarly to how v_1 and v_2 are used to obtain a dealiased velocity estimate in the staggered-PRT technique). However, this is not always feasible as shown in the next example. Figure 6 shows the ASD of a staggered-PRT weather

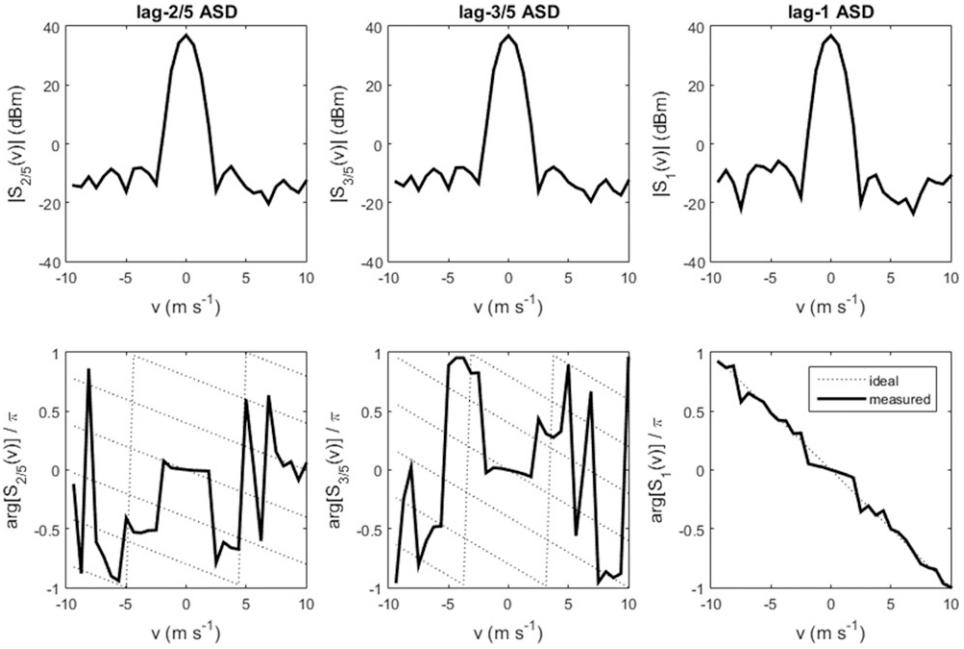

FIG. 4. As in Fig. 3, but for a simulated staggered-PRT sequence typical of ground clutter returns; the mean Doppler velocity is $0\,\mathrm{m\,s^{-1}}$ and the spectrum width is $0.28\,\mathrm{m\,s^{-1}}$.

signal with SNR = 40 dB, $\overline{v} = 0\,\mathrm{m\,s^{-1}}$, and $\sigma_v = 8\,\mathrm{m\,s^{-1}}$. In this case the spectral extent of the signal exceeds the Nyquist cointerval of $20\,\mathrm{m\,s^{-1}}$ dictated by T_s, and aliasing on the fractional-lag ASDs results in the incoherent addition of spectral components, a process that prevents robust identification of the proper Nyquist cointerval for effective dealiasing of the spectrum. That is, the phases of the fractional-lag ASDs do not lie on any of the theoretical lines. As expected, the limitations imposed by the spectrum width are the same as in the

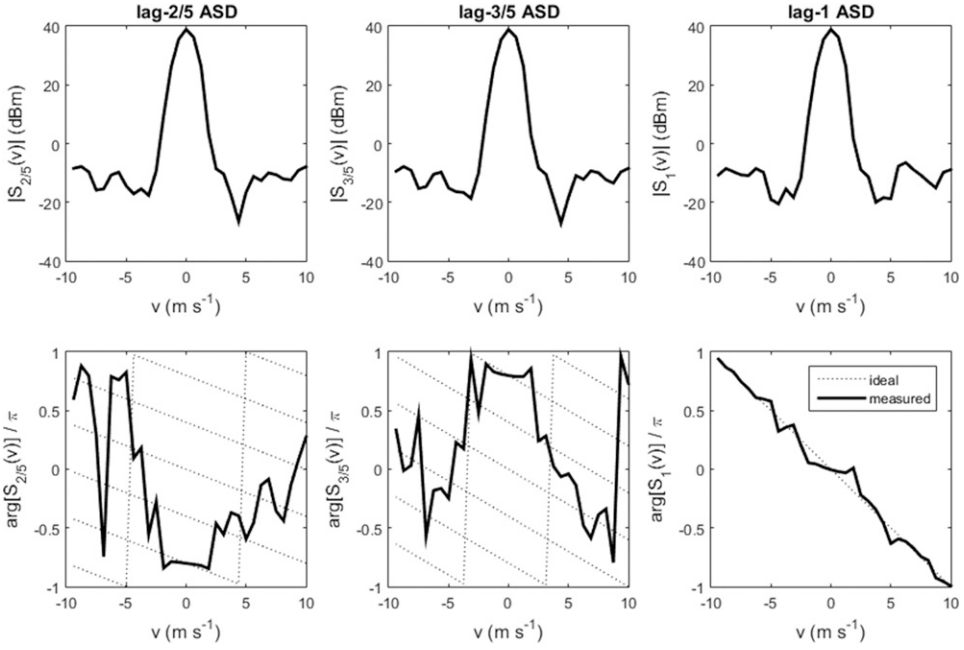

FIG. 5. As in Fig. 3, but the mean Doppler velocity is $20\,\mathrm{m\,s^{-1}}$ and the spectrum width is $0.28\,\mathrm{m\,s^{-1}}$.

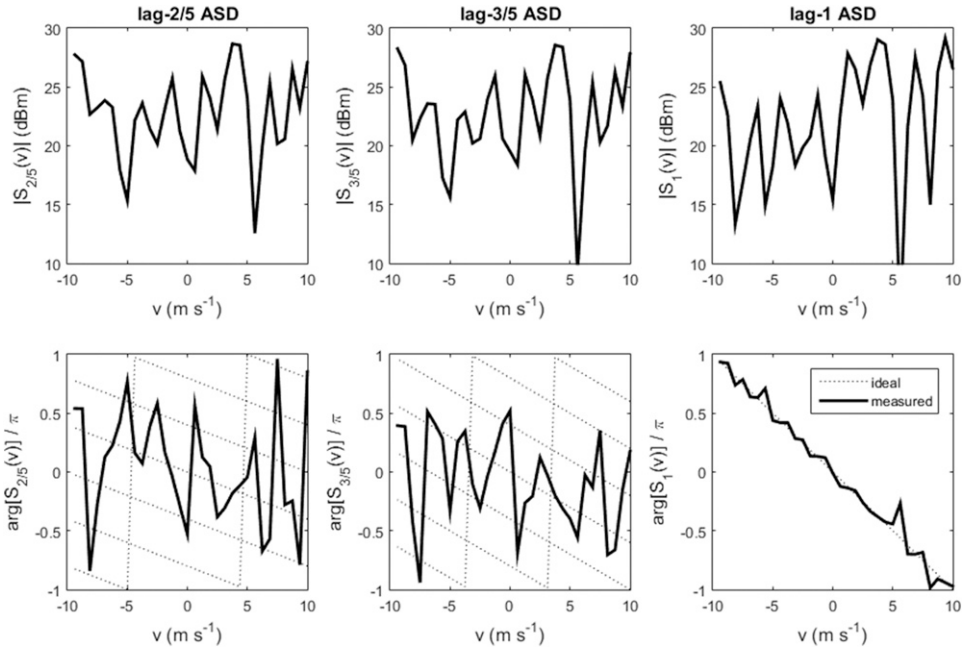

FIG. 6. As in Fig. 3, but the mean Doppler velocity is 0 m s^{-1} and the spectrum width is 8 m s^{-1}.

case of the PSD (Sachidananda and Zrnić 2000). That is, the ASD of staggered-PRT sequences is a better tool for spectral analysis when the spectral extent of the underlying uniformly sampled signal is less than $v_{a,s}$ as illustrated in the previous three examples.

Figures 7 and 8 show the ASD of a composite staggered-PRT signal containing weather and ground clutter returns. For the case in Fig. 7, the ground clutter signal has a clutter-to-noise (CNR) ratio of 40 dB, $\overline{v} = 0\,\mathrm{m\,s^{-1}}$, and $\sigma_v = 0.28\,\mathrm{m\,s^{-1}}$; and the weather signal

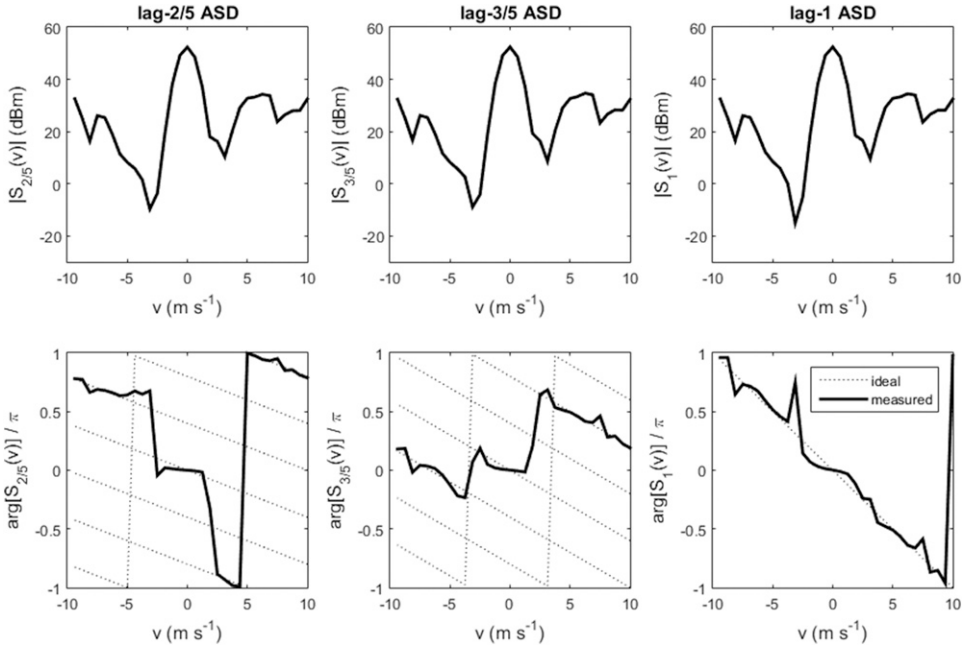

FIG. 7. As in Fig. 3, but for a composite signal typical of a ground clutter and weather mix. The parameters of the ground clutter signal are the same as in Fig. 4; for the weather signal, the SNR is 30 dB, the mean Doppler velocity is 28 m s^{-1}, and the spectrum width is 2 m s^{-1}.

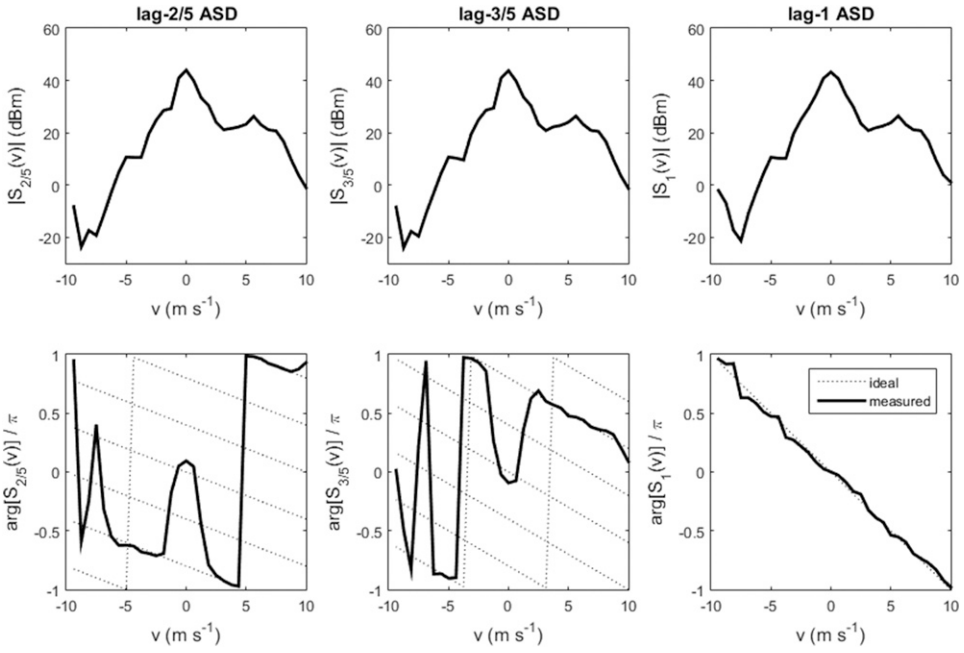

FIG. 8. As in Fig. 7, but for a weather signal with an SNR of 35 dB, a mean Doppler velocity of 22 m s^{-1}, and a spectrum width of 2 m s^{-1}.

has SNR = 30 dB, $\overline{v} = 28\,\mathrm{m\,s^{-1}}$, and $\sigma_v = 2\,\mathrm{m\,s^{-1}}$. These parameters are such that the ground clutter and weather spectra are minimally overlapped after aliasing. In this situation, the phases of the fractional-lag ASDs reveal that the two signals come from different Nyquist co-intervals. That is, the phases of the ASD around zero and 8 m s^{-1} velocities follow different theoretical curves and could be used to properly dealias the spectrum. Also, as expected, the ASD phases corresponding to the (narrowband) ground clutter signal are more biased, whereas the ones for the (wideband) weather signal are less so. Unlike this last case, the weather signal in Fig. 8 has SNR = 35 dB, $\overline{v} = 22\,\mathrm{m\,s^{-1}}$, and $\sigma_v = 2\,\mathrm{m\,s^{-1}}$, which result in significant overlap of the individual spectra after aliasing. Because the individual signal powers are about the same near 0 m s^{-1}, the ASD phases of the spectral coefficients with contributions from the two signals do not follow any of the theoretical curves. Outside this region, the phases are dominated by the stronger signal (the weather signal) and appear around their theoretical values. Similar to the signal in Fig. 6, the phase biases near 0 m s^{-1} due to aliasing prevent effective dealiasing but could provide a means to identify the presence of multiple signals in a given band of the aliased spectrum.

b. *Real data analysis*

Staggered-PRT data collected with the S-band KOUN radar (Norman, Oklahoma) at 2049 UTC 4 March 2004 is used next to illustrate spectral analysis using the ASD. Data corresponds to a large mesoscale convective system that moved from the south and resulted in strong winds and a severe thunderstorm warning for the area. For this case, $T_1 = 1.6$ ms, $T_2 = 2.4$ ms (the PRT ratio is 2/3), $M = 26$ (the total number of samples is 54), and the radar wavelength is 11.09 cm; thus, the unambiguous velocities corresponding to T_u and T_s ($v_{a,u}$ and $v_{a,s}$) are 34.7 and 6.94 m s^{-1}, respectively.

Figure 9 shows the magnitude (top panels) and phase (bottom panels) of the ASD at lags 2/5 (left panels), 3/5 (middle panels), and 1 (right panels) as a function of range (y axis) and (aliased) Doppler velocity (x axis) for a 2° ray centered at an azimuth angle of 138° and an elevation angle of 0.5°. To improve the readability of the plots, only range locations within 120 km from the radar are shown, and the spectra are smoothed with a 1-km range-averaging moving window. As expected, the magnitudes of the ASDs at all lags are very similar, and the phase of the lag-1 ASD is trivial. However, the phases of the ASDs at lags 2/5 and 3/5 reveal interesting information and can be used to dealias the spectra.

Figure 10 depicts the expected phase of the ASD at lags 2/5, 3/5, and 1 of a staggered-PRT weather signal with a 40-dB SNR, a 4 m s^{-1} spectrum width, and a mean Doppler velocity ranging from −34.7 to 34.7 m s^{-1} for the same acquisition parameters (PRTs and radar wavelength) used in the KOUN data. This figure provides a "key" for interpreting the ASD phases in

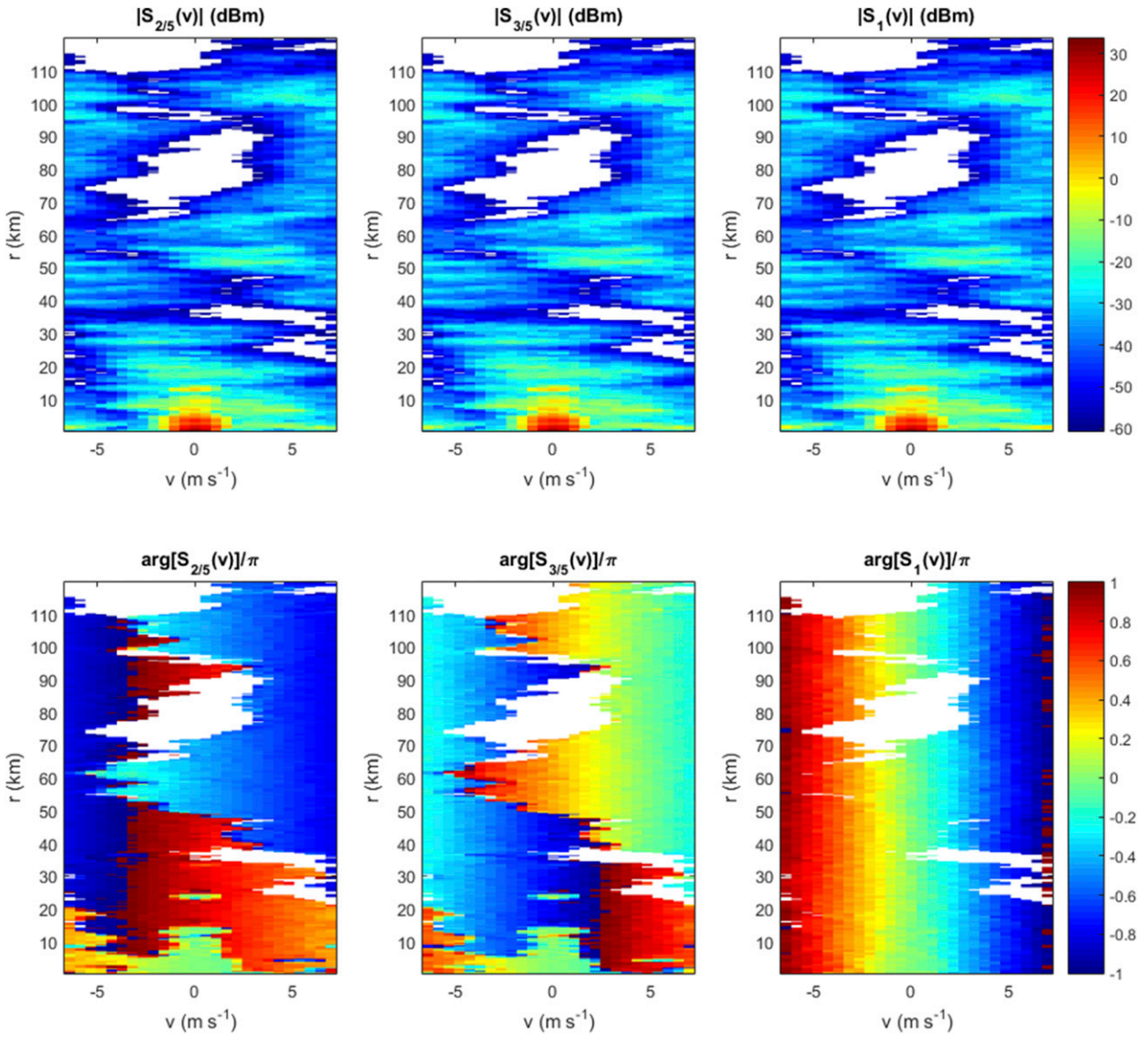

FIG. 9. ASD spectra corresponding to a ray of time series data collected with the KOUN radar at 2049 UTC 4 Mar 2004 as a function of Doppler velocity (x axis) and range (y axis). (top) Magnitude and (bottom) phase of the ASD at lags (left) 2/5, (center) 3/5, and (right) 1 are color coded and are shown for all range locations within 120 km of the radar. At each range location, there are 54 staggered-PRT samples with $T_1 = 1.6$ ms and $T_2 = 2.4$ ms. The range spacing is 250 m and $v_{a,s}$ is 6.9 m s^{-1}.

Fig. 9. For example, the ASD phases at lag 2/5 in Fig. 9 for (aliased) velocities around 0 m s^{-1} show mainly in light green (e.g., at ranges less than 15 km), in dark orange (e.g., between 25 and 35 km), or in light blue (e.g., between 50 and 70 km). From Fig. 10, it is easy to see that these colors correspond to true velocities in three different Nyquist cointervals: 0 (i.e., no aliasing), −13.9, and −27.76 m s^{-1}, respectively. Also, the ASD phases at lag 3/5 in Fig. 9 for (aliased) velocities around 5 m s^{-1} show mainly in red (e.g., at ranges less than 20 km), or in light green (e.g., between 40 and 120 km). From Fig. 10, these colors correspond to true velocities in two different Nyquist cointervals: −8.88 and −22.76 m s^{-1}, respectively. A similar analysis can be carried out for each spectral component and using ASD phases at either fractional lag.

As mentioned before, another advantage of using the ASD for spectral analysis is in its ability to identify strong narrowband signals such as those corresponding to ground clutter returns. Whereas ground clutter contamination is readily observed at ranges less than 10 km in both magnitude (higher values: yellow and red) and phase (near-zero values: light green), the ground clutter contamination at ~24 km is evident only in the phase of

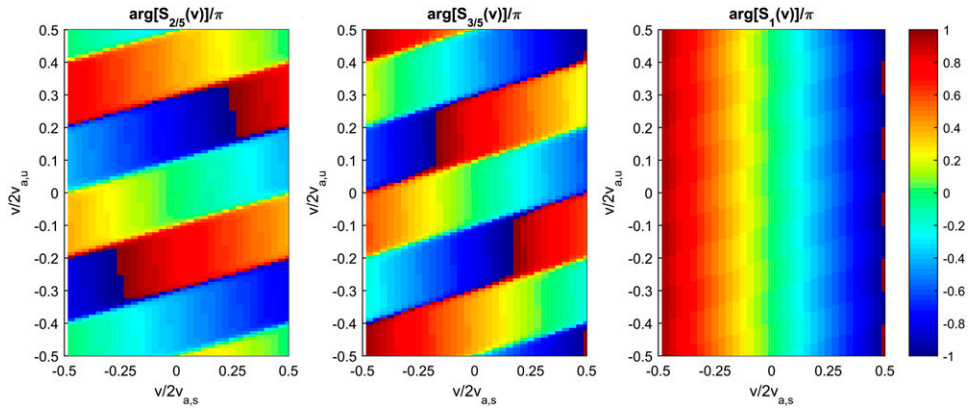

FIG. 10. Expected phase of the ASD at lags (left) 2/5, (center) 3/5, and (right) 1 for staggered-PRT weather signals with a 40-dB SNR, a 4 m s^{-1} spectrum width, a true mean Doppler velocity ranging from −34.7 to 34.7 (y axis), and the same acquisition parameters as the data in Fig. 9. Color patterns in this figure can be correlated with the phases in Fig. 9 to easily identify the correct Nyquist cointerval for all (aliased) spectral components of the data under analysis.

the ASD. Figure 11 shows the ASD spectra at this location similarly to Figs. 3–8, where it is evident that the spectral components near zero velocity correspond to the ground clutter signal (i.e., they exhibit near-zero ASD phases) and those away from zero velocity are aliased (i.e., they agree well with the theoretical phase line corresponding to the Nyquist cointerval between −13.88 and −27.76 m s^{-1}) and correspond to the weather signal.

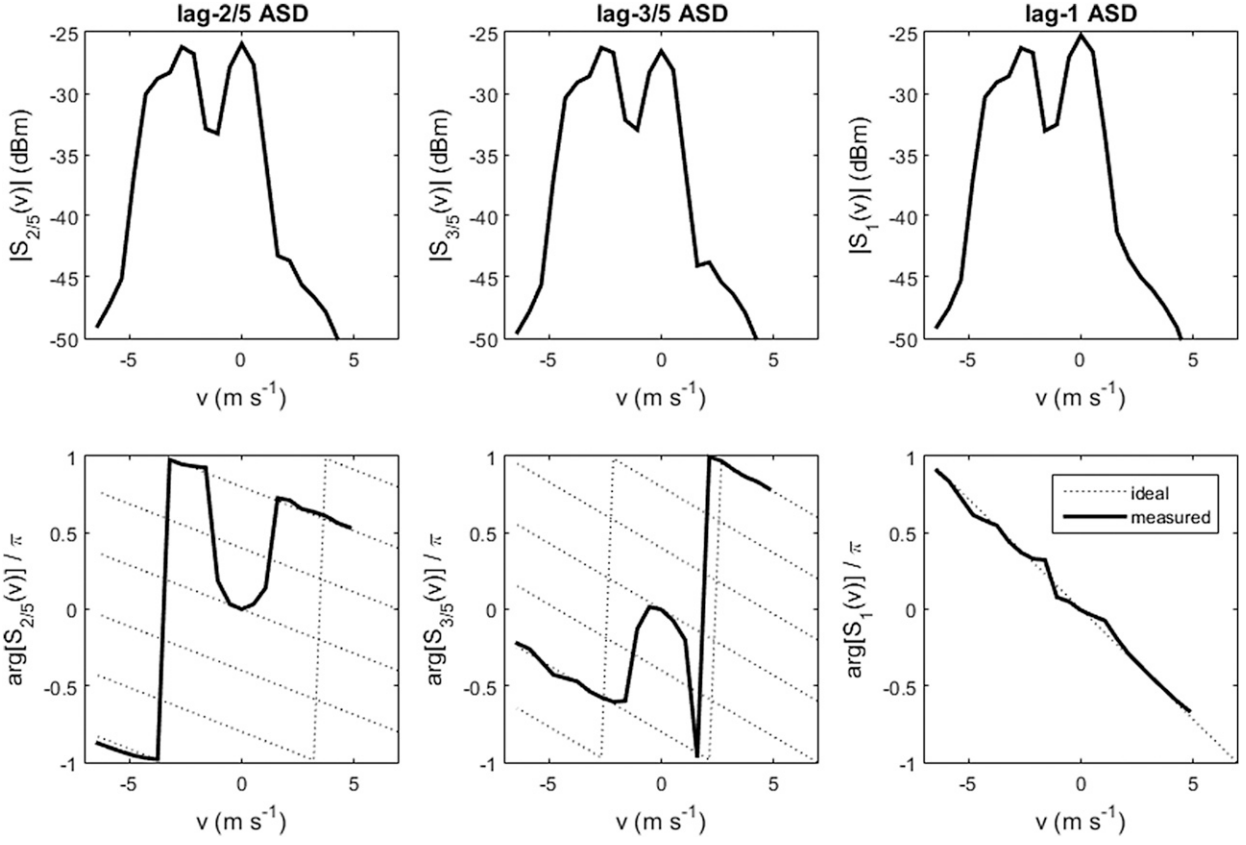

FIG. 11. As in Fig. 3, but for the real data in Fig. 9 at a range of ~24 km.

5. Conclusions

The autocorrelation spectral density (ASD) is an alternative tool for the spectral analysis of weather radar signals. In this paper, the ASD was applied to staggered pulse repetition time (PRT) sequences that use two alternating PRTs. The ASD of a staggered-PRT sequence was shown to be the aliased version of the ASD of the corresponding underlying uniform-PRT sequence. Thus, many of the uniform-PRT ASD properties directly apply or can be generalized. An ASD-based autocorrelation estimator was introduced and was shown to be unbiased and mathematically equivalent to the time-domain unbiased autocorrelation estimator when using a rectangular data window. The proposed ASD-based autocorrelation estimator can be used in the staggered-PRT algorithm in place of the traditional time-domain autocorrelation estimators. This is justified when performing spectral processing such as ground clutter filtering, which is the subject of Part II of this paper. The strengths and limitations of the ASD for spectral analysis of staggered-PRT sequences were illustrated using a few examples of simulated and real data. Like with uniform-PRT sequences, the phase of the ASD of staggered-PRT sequences provides a means to identify strong narrowband signals, such as those corresponding to ground clutter returns. Additionally, when the spectral extent of the signals under analysis is sufficiently narrow, the phase of the fractional-lag ASDs can be used to perform spectral dealiasing and to identify the presence of multiple signals in the spectrum. However, the usefulness of the ASD for spectral analysis of staggered-PRT sequences diminishes, as the spectral extent of the signals becomes too wide. Nevertheless, the ASD has the potential to improve the performance of operational weather radars by enabling the implementation of range and velocity ambiguity mitigation techniques based on the staggered-PRT sampling scheme. That is, the ASD can be at the core of an operational staggered-PRT algorithm that achieves larger maximum unambiguous velocities without a corresponding reduction in range coverage while maintaining the required levels of ground clutter suppression.

Acknowledgments. Funding was provided by NOAA/Office of Oceanic and Atmospheric Research under NOAA–University of Oklahoma Cooperative Agreement NA11OAR4320072, U.S. Department of Commerce.

REFERENCES

Cho, J. Y. N., 2005: Multi-PRI signal processing for the terminal Doppler weather radar. Part II: Range–velocity ambiguity mitigation. *J. Atmos. Oceanic Technol.*, **22**, 1507–1519, doi:10.1175/JTECH1805.1.

Chornoboy, E. S., and M. E. Weber, 1994: Variable-PRI processing for meteorological Doppler radars. *The Record of the 1994 IEEE National Radar Conference*, IEEE, 85–90, doi:10.1109/NRC.1994.328103.

Dazhang, T., S. G. Geotis, R. E. Passarelli Jr., A. L. Hansen, and C. L. Frush, 1984: Evaluation of an alternating-PRF method for extending the range of unambiguous Doppler velocity. Preprints, *22nd Conf. Radar Meteor.*, Zurich, Switzerland, Amer. Meteor. Soc., 523–527.

Doviak, R. J., and D. S. Zrnić, 1993: *Doppler Radar and Weather Observations*. Academic Press, 562 pp.

Fang, M., R. J. Doviak, and V. Melnikov, 2004: Spectrum width measured by WSR-88D: Error sources and statistics of various weather phenomena. *J. Atmos. Oceanic Technol.*, **21**, 888–904, doi:10.1175/1520-0426(2004)021<0888:SWMBWE>2.0.CO;2.

Hubbert, J. C., M. Dixon, and S. M. Ellis, 2009: Weather radar ground clutter. Part II: Real-time identification and filtering. *J. Atmos. Oceanic Technol.*, **26**, 1181–1197, doi:10.1175/2009JTECHA1160.1.

Moisseev, D. N., and V. Chandrasekar, 2009: Polarimetric spectral filter for adaptive clutter and noise suppression. *J. Atmos. Oceanic Technol.*, **26**, 215–228, doi:10.1175/2008JTECHA1119.1.

Oppenheim, A. V., and R. W. Schafer, 2009: *Discrete-Time Signal Processing*. 3rd ed. Prentice Hall, 1120 pp.

Pirttilä, J., M. S. Lehtinen, A. Huuskonen, and M. Markkanen, 2005: A proposed solution to the range–Doppler dilemma of weather radar measurements by using the SMPRF codes, practical results, and a comparison with operational measurements. *J. Appl. Meteor.*, **44**, 1375–1390, doi:10.1175/JAM2288.1.

Sachidananda, M., and D. S. Zrnić, 2000: Clutter filtering and spectral moment estimation for Doppler weather radars using staggered pulse repetition time (PRT). *J. Appl. Meteor.*, **17**, 323–331.

Sirmans, D., 1992: Clutter filtering in the WSR-88D. NWS/OSF Internal Rep., 125 pp. [Available from National Weather Service Radar Operations Center, 1200 Westheimer Dr., Norman, OK 73069.]

——, D. S. Zrnić, and W. Bumgarner, 1976: Estimation of maximum unambiguous Doppler velocity by use of two sampling rates. Preprints, *17th Conf. on Radar Meteorology*, Seattle, WA, Amer. Meteor. Soc., 23–28.

Tabary, P., L. Perier, J. Gagneux, and J. Parent-du-Chatelet, 2005: Test of a staggered PRT scheme for the French Radar Network. *J. Atmos. Oceanic Technol.*, **22**, 352–364, doi:10.1175/JTECH1709.1.

——, F. Guibert, L. Perier, and J. Parent-du-Chatelet, 2006: An operational triple-PRT Doppler scheme for the French radar network. *J. Atmos. Oceanic Technol.*, **23**, 1645–1656, doi:10.1175/JTECH1923.1.

Torres, S., and D. Warde, 2014: Ground clutter mitigation for weather radars using the autocorrelation spectral density. *J. Atmos. Oceanic Technol.*, **31**, 2049–2066, doi:10.1175/JTECH-D-13-00117.1.

——, Y. Dubel, and D. S. Zrnić, 2004: Design, implementation, and demonstration of a staggered PRT algorithm for the WSR-88D. *J. Atmos. Oceanic Technol.*, **21**, 1389–1399, doi:10.1175/1520-0426(2004)021<1389:DIADOA>2.0.CO;2.

——, R. Passarelli, A. Siggia, and P. Karhunen, 2010: Alternating dual-pulse, dual-frequency techniques for range and velocity ambiguity mitigation on weather radars. *J. Atmos. Oceanic Technol.*, **27**, 1461–1475, doi:10.1175/2010JTECHA1355.1.

Warde, D., and S. Torres, 2009: Range overlaid staggered PRT. Preprints, *25th Conf. on International Interactive Information and Processing Systems (IIPS) for Meteorology, Oceanography, and Hydrology (25IIPS)*, Phoenix, AZ, Amer. Meteor. Soc., P2.2. [Available online at https://ams.confex.com/ams/89annual/techprogram/paper_146269.htm.]

——, and ——, 2014: The autocorrelation spectral density for Doppler-weather-radar signal analysis. *IEEE Trans. Geosci. Remote Sens.*, **52**, 508–518, doi:10.1109/TGRS.2013.2241775.

——, ——, R. Ice, and A. Heck, 2014: Deployment of the staggered PRT algorithm on the NEXRAD network. *30th Conf. on Environmental Information Processing Technologies*, Atlanta, GA, Amer. Meteor. Soc., 5.4. [Available online at https://ams.confex.com/ams/94Annual/webprogram/Paper237155.html.]

Zrnić, D. S., 1975: Simulation of weatherlike Doppler spectra and signals. *J. Appl. Meteor.*, **14**, 619–620, doi:10.1175/1520-0450(1975)014<0619:SOWDSA>2.0.CO;2.